Journal of Zhejiang University-SCIENCE A (Applied Physics & Engineering)
ISSN 1673-565X (Print); ISSN 1862-1775 (Online)
www.zju.edu.cn/jzus; www.springerlink.com
E-mail: jzus@zju.edu.cn

Preliminary experimental study on solid-fuel rocket scramjet combustor

Zhong LV, Zhi-xun XIA[†‡], Bing LIU, Li-ya HUANG

(*Science and Technology on Scramjet Laboratory, National University of Defense Technology, Changsha 410073, China*)

[†]E-mail: zxxia@nudt.edu.cn

Received July 4, 2016; Revision accepted Aug. 22, 2016; Crosschecked Jan. 5, 2017

Abstract: Liquid or gaseous fuel scramjet technology has made great progress, and there has been some research attention to solid-fuel scramjet. A new scramjet configuration using solid fuel as propellant, namely solid-fuel rocket scramjet, is tested experimentally. It consists of two combustors. One is a rocket combustor used as gas generator, and the other is a supersonic combustor used for secondary combustion. The experiment simulates a flight Mach number of 4 at high altitude (stagnation temperature and pressure are 1170 K and 1.16 MPa, respectively), and metalized solid fuel is used as propellant. The results reveal that fuel-rich gas from the gas generator can burn with air in the supersonic combustor. Preliminary evaluation results show that the combustion efficiency of the propellant is about 90%, and the total pressure recovery coefficient in the supersonic combustor is about 0.6. These results indicate that the configuration of solid-fuel rocket scramjet is feasible.

Key words: Solid fuel; Rocket scramjet; Dual combustor; Direct-connect experiment
http://dx.doi.org/10.1631/jzus.A1600489 **CLC number:** V43

1 Introduction

The scramjet engine is one of most promising propulsion systems for hypersonic flight, and it attracts increasing attention (Fry, 2004). The main characteristics of the scramjet engine and its components have been studied comprehensively (Li *et al.*, 2008; Huang and Yan, 2013; Huang, 2014; 2015; Wang *et al.*, 2014; Yi and Chen, 2015; Huang *et al.*, 2016). Almost all studies on scramjet focus on liquid or gaseous fuel, and they demonstrate high energy, fast chemical kinetics, and good cooling properties. However, the use of solid fuel can decrease complexity and cost, and increase the energy density of the systems, which has advantages for certain missions. Some studies have been carried out on the solid-fuel scramjet, and they try to extend the use of the solid-fuel ramjet to the hypersonic flight range.

There are two basic types of ramjet utilizing solid-fuel propellant, namely the solid-fuel ramjet and the ducted rocket ramjet. The main studies on the solid-fuel scramjet focus on a configuration similar to the solid-fuel ramjet, as shown in Fig. 1. It pours the solid fuel into the combustor and makes the propellant burn directly in the supersonic airflow. Witt (1989) and Angus (1991) preliminarily validated the concept that solid fuel can burn in supersonic airflow, and initially determined the combustor configuration of the solid-fuel scramjet. Ben-Yakar *et al.* (1998) improved the configuration of the combustor. They demonstrated self-ignition and sustained combustion of solid fuel with no external aid. Saraf and Gany (2007) investigated the performance of a solid-fuel scramjet with metalized and non-metalized solid fuels. Wang *et al.* (2015) investigated the variation of the specific thrust during the operating process of the solid-fuel scramjet.

Those previous studies show the feasibility of the solid-fuel scramjet. However, they revealed some

[‡] Corresponding author
ORCID: Zhong LV, http://orcid.org/0000-0003-3741-3186; Zhi-xun XIA, http://orcid.org/0000-0002-2315-3005

operating problems:

1. Ignition and flame-holding is difficult in high-velocity airflow. The cavity used for ignition and flame-holding disappears as the burning surface regresses.

2. The mixing efficiency of fuel gases emerging from the wall with air diffusing from the core flow is low.

3. The chemical kinetic of the gasified hydrocarbon fuel may be slow compared with the residence time in supersonic flow.

4. The incomplete mixing and limited residence time make for a low combustion efficiency.

5. The overall fuel to air ratio cannot be controlled directly, and it is dependent on the fuel regression.

6. The internal configuration of the combustor varies with the fuel regression, and it will affect the performance of the scramjet engine.

Compared with the solid-fuel scramjet, the configuration of the ducted rocket ramjet may be easier to extend to the hypersonic flight range. In this paper, it is called the solid-fuel rocket scramjet, and its potential configuration is shown in Fig. 2.

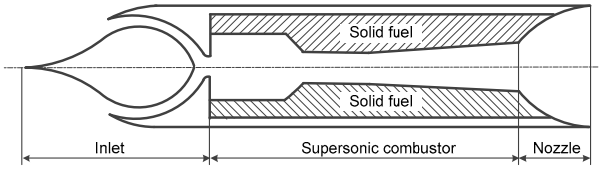

Fig. 1 Schematic of solid-fuel scramjet

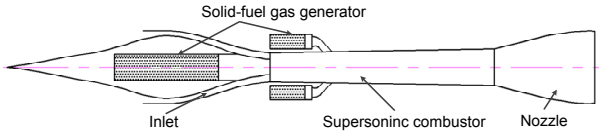

Fig. 2 Schematic of potential solid-fuel rocket scramjet

The solid-fuel rocket scramjet has two combustors. One is a gas generator, and the other is a supersonic combustor. The propellant first ignites and burns in the gas generator, and the high-temperature fuel-rich gas injects into the supersonic airflow and burns secondly with air. The ignition and flame-holding are easy to achieve. The secondary combustion can improve the combustion efficiency of the propellant. Since the mass flow rate of the fuel-rich gas can be controlled by the cross sectional area of a throat (Miller *et al.*, 1981), to some extent, the air to fuel rate in the engine can be controlled.

However, the static pressure and temperature in a scramjet combustor are much lower than that in a ramjet combustor. The key point of this configuration is whether the fuel-rich gas can mix and burn well with the supersonic airflow. In this paper, an experiment on the solid-fuel rocket scramjet combustor is conducted, and metalized solid fuel is used as propellant. The purpose of this study is to evaluate the feasibility of a solid-fuel rocket scramjet.

2 Experimental setup

The schematic of the direct-connected test facility is shown in Fig. 3. It consists of a vitiated air heater, a convergent-divergent nozzle, a tested combustor, and a data processing system. The vitiated air heater burns oxygen, ethanol, and air to simulate the stagnation parameters at the exit of inlet, which includes the total temperature (1170 K), the total pressure (1.16 MPa), and the oxygen mass concentration (0.233). The high-temperature gas from the vitiated air heater is accelerated to Mach number (*Ma*) of 1.65 by a convergent-divergent chocked nozzle. The mass flow rate of the vitiated air is about 9 kg/s.

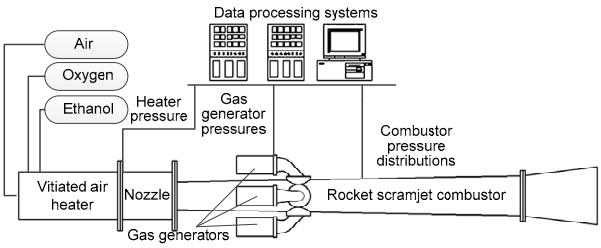

Fig. 3 Schematic of test facility

The tested solid-fuel rocket scramjet combustor consists of four solid-fuel gas generators, a supersonic combustor, and a nozzle, as shown in Fig. 4. The supersonic combustor and the nozzle are two diverging ducts, and the divergent angles are 1° and 3°, respectively. The diameter at the entrance of the combustor (d) is set as the reference parameter, and the length of the supersonic combustor and nozzle are 13.4d and 2.6d, respectively. Four solid-fuel gas generators are assembled around the supersonic

combustor, and the distance is 4.6*d* from the entrance of the combustor. The injection angle is 45° from the axial line.

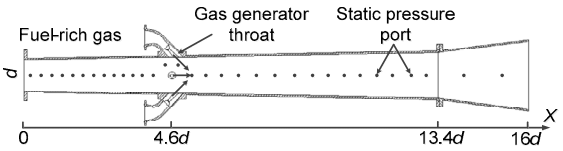

Fig. 4 Schematic of the tested combustor

The propellant employed here is a metalized solid fuel. It contains a large amount of magnesium powder and a small amount of binder and oxidant. The mass content of the magnesium is 50%. The burn rate of the propellant is about 13 mm/s. The propellant is made into end-burning grain with a diameter of 60 mm, and it is the same as the internal chamber diameter of the solid-fuel gas generator. The nozzle throat diameter of the gas generator is 11 mm. The mass flow rate of the fuel-rich gas can be calculated by

$$\dot{m}_{\mathrm{p}} = \alpha p_{\mathrm{SFGG}}^{n} \rho_{\mathrm{p}} A_{\mathrm{p}}, \tag{1}$$

where α is the burn rate coefficient, n is the pressure exponent, and both depend on the component of the propellant. p_{SFGG} is the pressure in the solid fuel gas generator, ρ_{p} is the density of the propellant, and A_{p} is the cross sectional area of the propellant.

A total of 33 pressure-tap ports are distributed on the wall of the supersonic combustor and nozzle, as shown in Fig. 4. Each port is connected to the intelligent pressure scanner (model 9116 of Pressure System Inc., USA, accuracy ±0.05%) to measure the pressure distribution along the wall. The maximum sampling frequency of the pressure scanner is 500 Hz, and the accuracy is about ±0.05% of the full scale (689.5 kPa in this experiment). Five piezoresistive pressure transducers, ranging from 0 to 5 MPa with an error of 0.05% of full scale, are used to measure the pressure of gas generators and the vitiated air heater. Mass flow rates of the gas are measured by turbo flow meters, and the accuracy of the flow meters is about ±0.2% of the full scale. All the data from the sensors are transmitted to a PCI extensions for instrumentation (PXI) measurement system through high speed Ethernet, and the PXI system is connected with the control system to diagnose the real-time status.

3 Results and discussion

The study contains two experiments. One is a solid-fuel gas generator experiment, and the other is a solid-fuel rocket scramjet combustor experiment. The former is used to test the performance of the propellant, and the latter is used to test the performance of the solid-fuel rocket scramjet combustor.

In the gas generator experiment, the solid-fuel gas generator was tested alone, and the vitiated air heater was not working. The temporal evolution of pressure in the gas generator is shown in Fig. 5. The propellant is ignited by the ignitor, and a peak pressure of 2 MPa is obtained. The pressure in the gas generator continues to increase until all of the propellant is burned out.

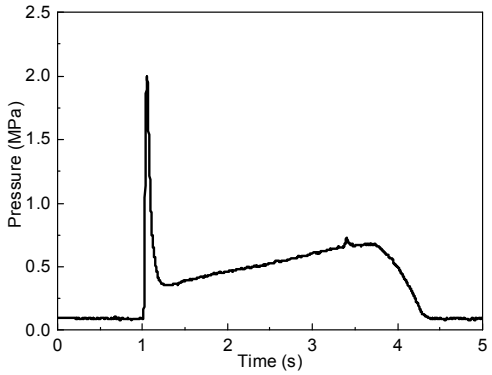

Fig. 5 Temporal evolution of pressure in gas generator

Fig. 6 shows the picture of the gas generator throat after the experiment. It is obvious that some initial-combustion products freeze on the surface of the throat. The thickness of deposition is about 1 mm. X-ray diffraction analysis indicates that the deposition mainly consists of magnesium, carbon, and a

Fig. 6 Picture of throat after experiment

little magnesium oxide. The deposition decreases the diameter of the throat and results in the pressure rise in the gas generator.

In the solid-fuel rocket scramjet combustor experiment, the vitiated air heater begins to work at about 4.0 s, and it operates steadily 0.5 s later, as shown in Fig. 7. The propellant ignites at 5.5 s and the peak pressure is about 2.1 MPa. After ignition, the pressure in the gas generator increases slowly until all of the propellant burns out.

Fig. 8 presents a video photograph of the combustion flame at the exit of the nozzle. The image reveals that the fuel-rich gas injected from the gas generator can burn continually with air in the supersonic combustor. Brilliant-white light exists in the center of the combustion flame, and this is produced from the combustion of magnesium. The red light in the peripheral area is produced from the combustion of hydrocarbons, and the white smoke downstream is composed primarily of magnesium oxide.

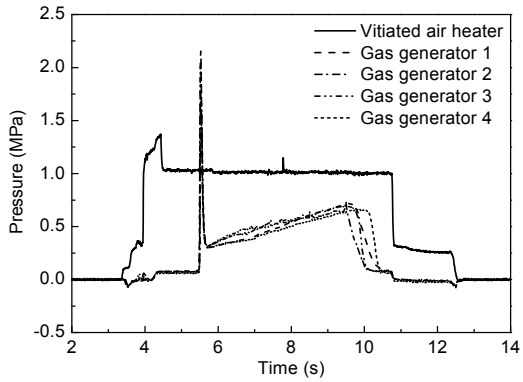

Fig. 7 Temporal evolution of pressures in the vitiated air heater and gas generators

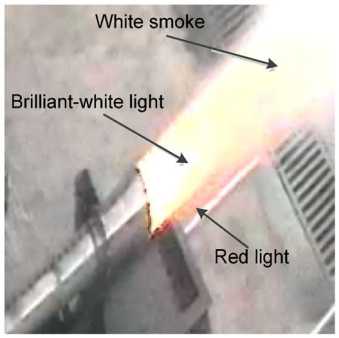

Fig. 8 Image of combustion flame at the exit of the nozzle
Note: for interpretation of the references to color in this figure legend, the reader is referred to the web version of this article

The pressure in the gas generator increases with time, and this is the same in the gas generator experiment. However, the outlet pressure of the gas generator is not constant, and it changes with the pressure in the supersonic combustor (see X=500 mm in Fig. 9). The pressure ratio is slightly lower than the critical value. Thus, the pressure in the combustor will affect the pressure in the gas generator. However, it is not the main reason for the pressure rise in the gas generator. The comparison of Fig. 5 with Fig. 7 indicates that the deposition is the main reason.

Fig. 9 presents the pressure distribution along the supersonic combustor. Before ignition, pressure decreases along the combustor for the expansion of the sectional area of the combustor. The pressure at the exit of the nozzle is lower than that of the environment. The pressure does not rise in the nozzle, and that means the pressure in the environment does not affect the air-flow in the nozzle.

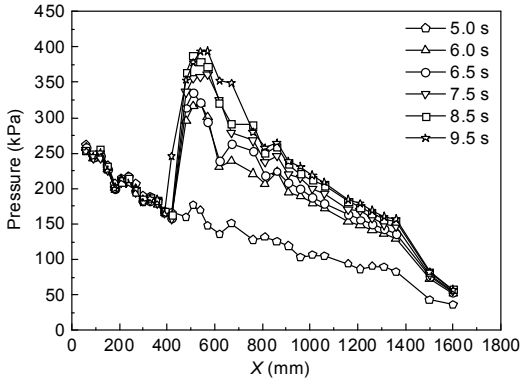

Fig. 9 Pressure distributions along the wall at different times (t) (X is the distance from the combustor entrance)

After ignition, the pressure in the vicinity of the fuel injection increases. The process of fuel-rich gas injected into the supersonic combustor is a typical single, under-expanded, transverse jet in a supersonic flow (Glagolev *et al.*, 1967; 1968; Brieschenk *et al.*, 2013). The jet forms a blockage for the incoming supersonic flow, thus resulting in the generation of a bow shock, which leads to boundary-layer separation and the formation of a recirculation region in front of the jet. The pressure rise in the vicinity of the fuel injection is induced for two reasons. One is the compression of the bow shock induced by the fuel injection, and the other is the heat addition of the fuel-rich gas. The heat addition consists of two parts. One is the

heat taken from the high-temperature fuel-rich gas, and the other is the heat release from secondary combustion of the fuel-rich gas with air. Since some initial steps of combustion have taken place in the gas generator, the combustion can occur quickly as the fuel-rich mixes well with air.

As time goes on, the pressure distribution along the supersonic combustor rises overall. Because of the deposition, the pressure in the gas generator increases with time, and the mass flow rate of fuel-rich gas also increases, as shown in Eq. (1). More fuel-rich gas is injected into the supersonic airflow, and this results in the pressure rise overall, especially in the vicinity of the fuel injection. The point that the pressure begins to rise translates upstream (see t=9.5 s in Fig. 9). As the pressure increases in the combustor, the adverse pressure gradient near the fuel injection increases. When the adverse pressure gradient increases to some extent, the pressure will translate upstream along the boundary layer. The separation shock wave induced by the separated boundary-layer translates upstream, resulting in the translation upstream of the point that the pressure begins to rise.

To obtain more flow properties along the supersonic combustor, the wall pressure (p_w) distribution is used with a quasi-one-dimensional analysis approach proposed by Curran and Murthy (2000). The approach is based on the following equations for Mach number (Ma) and the total temperature (T_t):

$$\frac{\mathrm{d}Ma}{Ma}=\frac{1}{Ma^2-1}\left(1+\frac{\gamma-1}{2}Ma^2\right)\times\left[\frac{\mathrm{d}A}{A}-\frac{\gamma Ma^2+1}{2}\frac{\mathrm{d}T_t}{T_t}-\frac{Ma^2}{2}\times 4C_f\frac{\mathrm{d}x}{D}\right], \quad (2)$$

$$\frac{\mathrm{d}T_t}{T_t}=\frac{1}{1+(\gamma-1)Ma^2/2}\times\left[\frac{Ma^2-1}{\gamma Ma^2}\frac{\mathrm{d}p_w}{p_w}+\frac{\mathrm{d}A}{A}-\frac{1+(\gamma-1)Ma^2}{2}\times 4C_f\frac{\mathrm{d}x}{D}\right], \quad (3)$$

where C_f is the skin friction coefficient, and it is estimated by the van Driest method (van Driest, 2003). γ is the ratio of specific heat, A is the cross-sectional area of the combustor duct, and D is the hydraulic diameter. The equations are solved by the fourth-order Ronge-Kutta method. Therefore, the Mach number and the total temperature distributions are calculated (Yu *et al.*, 1998; Bao *et al.*, 2013). The total pressure distribution p_t can be calculated by

$$p_t=p\left[\frac{1+(\gamma-1)Ma^2}{2}\right]^{\frac{\gamma}{\gamma-1}}. \quad (4)$$

The Mach number distributions along the supersonic combustor with different times are shown in Fig. 10. Mach number clearly decreases in the vicinity of the fuel injection. This is induced for two reasons. One is the compression of the shock wave, and the other is heat release of the fuel-rich gas. These two processes also cause a large total pressure loss. The total pressure loss in the supersonic combustor is mainly located in the region in the vicinity of fuel injection, as shown in Fig. 11. The total pressure after the position of fuel injection is lower than that in the vicinity of fuel injection, and the total pressure decreases as the increase of mass flow rate of fuel-rich gas. The fuel-rich gas injected from the gas generator is at high temperature, and the secondary combustion takes place quickly in the vicinity of the fuel injection, so it is easy to form a thermal throat at this region after fuel injection (see t=9.5 s, X around 500 mm in Fig. 10).

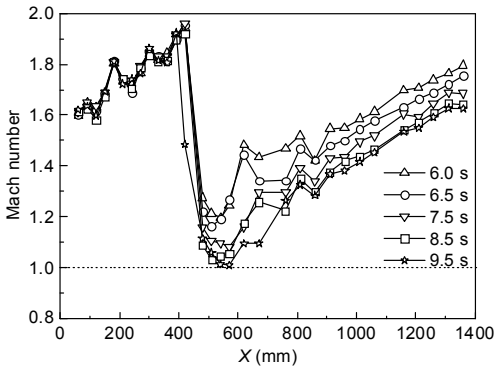

Fig. 10 Mach number distributions along the wall with different times

To evaluate the overall performance of the supersonic combustor, two parameters, namely total pressure recovery coefficient π and combustion efficiency η, are employed. The total pressure recovery coefficient is defined as the ratio of the total pressures between the exit ($p_{t,e}$) and the entrance ($p_{t,in}$) of the supersonic combustor, as shown in Eq. (5). The total

pressure at the entrance is measured in the experiment. The combustion efficiency is defined based on the temperature rise, as shown in Eq. (6), and the theoretical total temperature at the exit ($T_{t,e,th}$) and the entrance ($T_{t,in}$) of the supersonic combustor are calculated by the National Aeronautics and Space Administration (NASA)'s chemical equilibrium with application (CEA) program (Gordon and McBride, 1994).

$$\pi = \frac{p_{t,e}}{p_{t,in}}, \tag{5}$$

$$\eta = \frac{T_{t,e} - T_{t,in}}{T_{t,e,th} - T_{t,in}}. \tag{6}$$

Both the total pressure ($p_{t,e}$) and temperature ($T_{t,e}$) at the exit are calculated by the quasi-one dimensional model. Though the data calculated by the quasi-one dimensional model is not quite accurate, it can be used to evaluate approximately the performance of the supersonic combustor. More refined data should be tested in further study.

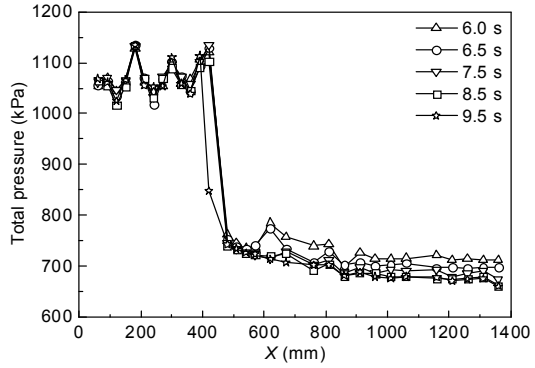

Fig. 11 Total pressure distributions along the wall at different times

The total pressure recovery coefficient is about 0.6, and the combustion efficiency of the propellant is about 90%. The total temperature calculated based on the pressure data is about 1753 K, and the theoretical total temperature calculated by CEA is 1821 K. If the fuel-rich gas just mixes and does not burn with the air, the total temperature calculated by CEA is 1190 K, which is much lower than that calculated based on the pressure data. This also reveals that the fuel-rich gas can burn with air in a supersonic combustor, and the configuration of the solid-fuel scramjet is feasible.

4 Conclusions

An experimental study of the solid-fuel rocket scramjet combustor is conducted. The results are summarized as follows:

1. Fuel-rich gas from gas generation can burn with the air in the supersonic combustor, and the configuration of the solid-fuel scramjet is feasible.

2. A preliminary evaluation of the performance of the solid-fuel rocket scramjet is carried out. The total pressure recovery coefficient in the supersonic combustor is about 0.6, and the combustion efficiency of the propellant is about 90%.

3. Some initial-combustion products freeze on the surface of the throat of gas generator, which decreases the diameter of the throat and results in the pressure rise in the gas generator. It also induces the increase of mass flow rate of fuel-rich gas.

4. The total pressure loss is mainly located in the region in the vicinity of the fuel-rich gas injection. The loss is mainly induced by the shock waves resulting from fuel injection and the secondary combustion of the fuel-rich gas with air.

References

Angus, W.J., 1991. An Investigation into the Performance Characteristics of a Solid Fuel Scramjet Propulsion Device. MS Thesis, Naval Postgraduate School, Monterey, USA.

Bao, W., Yang, Q.C., Chang, J.T., *et al.*, 2013. Dynamic characteristics of combustion mode transitions in a strut-based scramjet combustor model. *Journal of Propulsion and Power*, **29**(5):1244-1248. http://dx.doi.org/10.2514/1.B34921

Ben-Yakar, A., Natan, B., Gany, A., 1998. Investigation of a solid fuel scramjet combustor. *Journal of Propulsion and Power*, **14**(4):447-455. http://dx.doi.org/10.2514/2.5321

Brieschenk, S., O'Byrne, S., Kleine, H., 2013. Laser-induced plasma ignition studies in a model scramjet engine. *Combustion and Flame*, **160**(1):145-148. http://dx.doi.org/10.1016/j.combustflame.2012.08.011

Curran, E.T., Murthy, S.N.B., 2000. Scramjet Propulsion. The American Institute of Aeronautics and Astronautics, Reston, USA, p.588-593.

Fry, R.S., 2004. A century of ramjet propulsion technology

evolution. *Journal of Propulsion and Power*, **20**(1):27-58. http://dx.doi.org/10.2514/1.9178

Glagolev, A.I., Zubkov, A.I., Panov, Y.A., 1967. Supersonic flow past a gas jet obstacle emerging from a plate. *Fluid Dynamics*, **2**(3):60-64. http://dx.doi.org/10.1007/BF01027359

Glagolev, A.I., Zubkov, A.I., Panov, Y.A., 1968. Interaction between a supersonic flow and gas issuing from a hole in a plane. *Fluid Dynamics*, **3**(2):99-103.

Gordon, S., McBride, B.J., 1994. Computer Program for Calculation of Complex Chemical Equilibrium Compositions and Applications, I. Analysis. NASA Reference Publication, USA.

Huang, W., 2014. Design exploration of three-dimensional transverse jet in a supersonic crossflow based on data mining and multi-objective design optimization approaches. *International Journal of Hydrogen Energy*, **39**(8):3914-3925. http://dx.doi.org/10.1016/j.ijhydene.2013.12.129

Huang, W., 2015. A survey of drag and heat reduction in supersonic flows by a counterflowing jet and its combinations. *Journal of Zhejiang University-SCIENCE A (Applied Physics & Engineering)*, **16**(7):551-561. http://dx.doi.org/10.1631/jzus.A1500021

Huang, W., Yan, L., 2013. Progress in research on mixing techniques for transverse injection flow fields in supersonic crossflows. *Journal of Zhejiang University-SCIENCE A (Applied Physics & Engineering)*, **14**(8):554-564. http://dx.doi.org/10.1631/jzus.A1300096

Huang, W., Li, M.H., Ding, F., *et al*., 2016. Supersonic mixing augmentation mechanism induced by a wall-mounted cavity configuration. *Journal of Zhejiang University-SCIENCE A (Applied Physics & Engineering)*, **17**(1):45-53. http://dx.doi.org/10.1631/jzus.A1500244

Li, J.P., Song, W.Y., Xing, Y., *et al*., 2008. Influences of geometric parameters upon nozzle performances in scramjets. *Chinese Journal of Aeronautics*, **21**(6):506-511. http://dx.doi.org/10.1016/S1000-9361(08)60167-3

Miller, W., McClendon, S., Burkes, W., 1981. Design approaches for variable flow ducted rockets. 17th Joint Propulsion Conference, Colorado Springs, USA. http://dx.doi.org/10.2514/6.1981-1489

Saraf, S., Gany, A., 2007. Testing metalized solid fuel scramjet combustor. 18th International Symposium on Air Breathing Engines, p.1176-1187.

van Driest, E.R., 2003. Turbulent boundary layer in compressible fluid. *Journal of Spacecraft and Rockets*, **40**(6):1012-1028. http://dx.doi.org/10.2514/2.7048

Wang, L.H., Wu, Z.W., Chi, H.W., *et al.*, 2015. Numerical and experimental study on the solid-fuel scramjet combustor. *Journal of Propulsion and Power*, **31**(2):685-693. http://dx.doi.org/10.2514/1.B35302

Wang, Z.G., Wang, H.B., Sun, M.B., 2014. Review of cavity-stabilized combustion for scramjet applications. *Proceedings of the Institution of Mechanical Engineers, Part G: Journal of Aerospace Engineering*, **228**(14):2718-2735. http://dx.doi.org/10.1177/0954410014521172

Witt, M.A., 1989. Investigation into the Feasibility of Using Solid Fuel Ramjets for High Supersonic Low Hypersonic Tactical Missiles. MS Thesis, Naval Postgraduate School, Monterey, USA.

Yi, S.H., Chen, Z., 2015. Review of recent experimental studies of the shock train low field in the isolator. *Acta Physica Sinica*, **64**(19):0199401 (in Chinese). http://dx.doi.org/10.7498/aps.64.199401

Yu, G., Li, J.G., Zhao, J.R., *et al.*, 1998. Hydrogen-air supersonic combustion study by strut injectors. 34th AIAA/ASME/SAE/ASEE Joint Propulsion Conference and Exhibit. http://dx.doi.org/10.2514/6.1998-3275

中文概要

题　目：固体火箭超燃冲压发动机燃烧室初步实验研究

目　的：通过发动机直连式实验，验证燃气发生器产生的富燃燃气可以在超声速气流中二次燃烧，进而证明固体火箭超燃冲压发动机方案的可行性，并初步评估固体火箭超燃冲压发动机燃烧室的工作性能。

创新点：1. 提出固体火箭超燃冲压发动机构型方案，并开展固体火箭超燃冲压发动机燃烧室直连式实验研究；2. 验证了固体火箭超燃冲压发动机构型可行；3. 初步评估了固体火箭超燃冲压发动机燃烧室的工作性能。

方　法：1. 通过直连式实验测定固体火箭超燃冲压发动机燃烧室的工作参数（图 2、3 和 4）；2. 通过实验现象（图 8）和数据处理，确定燃气发生器产生的富燃燃气可以在超声速燃烧室中燃烧，进而确定固体火箭超燃冲压发动机方案的可行性；3. 初步确定发动机燃烧室的工作性能（公式（6）和（7））。

结　论：1. 燃气发生器中产生的富燃燃气可以在超声速燃烧室中燃烧，固体火箭超燃冲压发动机构型方案可行；2. 初步评估了固体火箭超燃冲压发动机燃烧室的工作性能，总压恢复系数约为 0.6，燃烧效率约为 90%；3.燃气发生器产生的部分一次燃气沉积于燃气发生器喉部，使燃气发生器的工作压力增加，进而引起富燃燃气质量流量的增加；4. 燃烧室中的总压损失主要集中在富燃燃气入口处，总压损失主要由射流引起的激波和燃气二次燃烧引起。

关键词：固体燃料；火箭超燃冲压发动机；双燃烧室；直连式实验